

# Group velocity control in the ultraviolet domain via interacting dark-state resonances

Mohammad Mahmoudi<sup>1,2</sup>, Mostafa Sahrai<sup>3</sup>, and Jörg Evers<sup>1</sup>

<sup>1</sup>Max-Planck-Institut für Kernphysik, Saupfercheckweg 1, D-69117 Heidelberg, Germany

<sup>2</sup>Physics Department, Zanzan University, P. O. Box 45195-313, Zanzan, Iran

<sup>3</sup>Research Institute for Applied Physics and Astronomy, University of Tabriz, Tabriz, Iran

**Abstract.** The propagation of a weak probe field in a laser-driven four-level atomic system is investigated. We choose mercury as our model system, where the probe transition is in the ultraviolet region. A high-resolution peak appears in the optical spectra due to the presence of interacting dark resonances. We show that this narrow peak leads to superluminal light propagation with strong absorption, and thus by itself is only of limited interest. But if in addition a weak incoherent pump field is applied to the probe transition, then the peak structure can be changed such that both sub- and superluminal light propagation or a negative group velocity can be achieved without absorption, controlled by the incoherent pumping strength.

## 1. Introduction

Optical properties of an atomic medium can be substantially modified by the application of external fields. In particular, atomic coherence induced by laser fields plays an important role in light-matter interaction and has found numerous implementations in optical physics [1]. One prominent application is the modification of the propagation of a light pulse through an atomic medium, which depends on the dispersive properties of the medium. The study of such pulse propagation phenomena has been triggered by a series of papers by Sommerfeld and Brillouin [2, 3] and continues to be of much interest [4, 5, 6, 7, 8, 9]. It is well known that the group velocity of a light pulse can be slowed down [10, 11], can become faster than its value  $c$  in vacuum, or can even become negative [12, 13]. Note that superluminal light propagation with group velocity larger than  $c$  cannot transmit information faster than the vacuum speed of light [14], such that it is not at odds with causality. Superluminal light propagation has been investigated for many potential uses, not only as a tool for studying a very peculiar state of matter, but also for developing quantum computers, high speed optical switches and communication systems [15].

Both experimental and theoretical studies have been performed to realize super- and subluminal light propagation in a single system. For example, speed control in atomic systems has been achieved by changing the frequencies, amplitudes or phase differences of the applied fields. It has been shown that switching from subluminal to superluminal pulse propagation can be achieved by the intensity of the coupling fields [16, 17, 18, 19], and the relative phase between two weak probe fields [20]. Morigi et al. [21] have compared the phase-dependent properties of the  $\diamond$  (diamond) four level system with those of the double  $\Lambda$  system. In Ref. [13], gain-assisted superluminal light propagation was observed in a cesium vapor cell while in most other studies, superluminal light propagation is accompanied by considerable absorption. Sub- and superluminal light propagation together with nonlinear optical gain or losses were observed in [22]. Two of the present authors suggested to use an incoherent pump field to control light propagation from subluminal to superluminal [23, 24]. Recently, we have studied the light propagation of a probe pulse in a four-level double lambda system, where the applied laser fields form a closed interaction loop [25]. In such systems, the finite frequency width of a probe pulse requires a time dependent treatment of the light propagation. We have found both sub- and superluminal light propagation without absorption or with gain, controlled by the Rabi frequency of one of the coupling fields.

All these effects depend on the modification of the dispersive and absorptive properties of the atomic medium. A particular class of systems that allows to modify the optical response to a great extent are those with so-called interacting dark resonances [26]. A characteristic feature of such systems is the appearance of very sharp, high-contrast structures in the optical spectra. Resonances associated with double dark states can be made absorptive or transparent and their optical properties such as width and position can be manipulated by applying suitable coherent interactions. It was

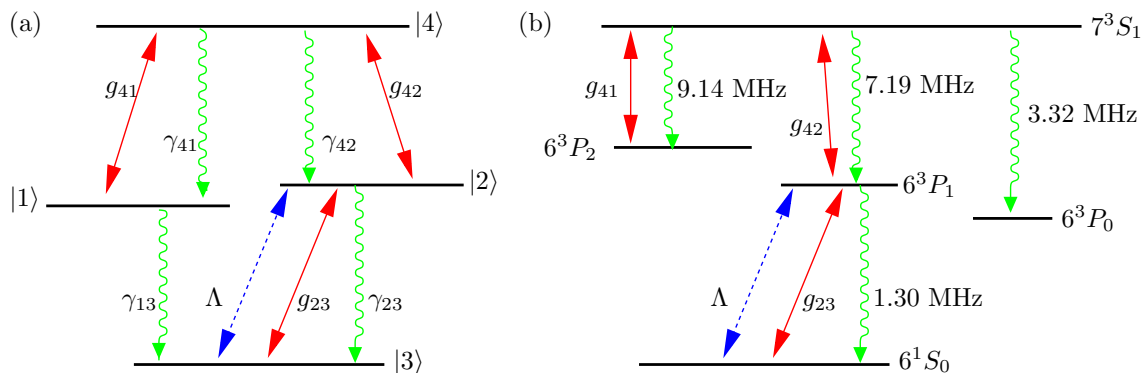


**Figure 1.** (a) Energy scheme of the four level atomic system considered. Transition  $|2\rangle \leftrightarrow |4\rangle$  is driven by a strong laser field, transition  $|1\rangle \leftrightarrow |4\rangle$  by a weak coupling field, and the probe field interacts with transition  $|2\rangle \leftrightarrow |3\rangle$ . In addition, a weak incoherent field is applied to the probe field transition. (b) A possible realization of the scheme in mercury. Population transfer to state  $6^3P_0$  has to be compensated via a repump field.

also shown that very weak incoherent excitation of the atoms can be sufficient to turn absorptive features into optical gain structures. This has been proposed as a model system to obtain strong laser gain in the ultraviolet and vacuum ultraviolet regime by Fry et al. [27].

In this paper we consider probe pulse propagation through a system which exhibits interacting dark resonances. The level configuration of our four-level scheme is based on the lasing system proposed in [27], and consists of three atomic states in ladder configuration, with an additional fourth perturbing state coupled by a laser field to the upper state of the ladder system. The lower transition of the ladder system acts as the probe transition. This system can be realized, e.g., in mercury, where the probe transition has a low wavelength of 253.7 nm, i.e., in the ultraviolet region. We find that the medium susceptibility in dependence on the probe field detuning exhibits high-contrast structures characteristic of interacting dark states. These structures typically lead to superluminal probe field propagation with high absorption, and thus as such are of limited interest. If, however, a weak incoherent pumping is applied in addition to the probe field transition, then we find that in the region around a narrow structure both sub- and superluminal propagation as well as negative group velocities are possible without absorption, controlled by the incoherent pumping strength.

## 2. Analytical considerations

### 2.1. The Model System

We consider an atomic four level system as shown in figure 1(a). Transition  $|2\rangle \leftrightarrow |4\rangle$  is driven by a strong coherent field with frequency  $\omega_{42}$  and Rabi frequency  $g_{42}$ . A weak coupling field with frequency  $\omega_{41}$  and Rabi frequency  $g_{41}$  is applied to transition  $|1\rangle \leftrightarrow |4\rangle$ . The weak probe field with frequency  $\omega_{23}$  and Rabi frequency  $g_{23} = g_p$  couples

to transition  $|2\rangle \leftrightarrow |3\rangle$ . Finally, an incoherent driving field with pump strength  $\Lambda$  is applied to the probe transition. We further include spontaneous decay with rates  $\gamma_{41}$ ,  $\gamma_{42}$ ,  $\gamma_{23}$ , and  $\gamma_{13}$ , respectively, on the dipole-allowed transitions. The atomic transition frequencies are denoted by  $\bar{\omega}_{ij}$ , and the laser field detunings with respect to the atomic transition frequencies are  $\Delta_{ij} = \omega_{ij} - \bar{\omega}_{ij}$  ( $i, j \in 1, \dots, 4$ ). A realization of our level scheme can be found, e.g., in mercury, see figure 1(b).

The density matrix equations of motion, in the rotating wave approximation, are

$$\dot{\rho}_{11} = -2\gamma_{13}\rho_{11} + 2\gamma_{41}\rho_{44} - ig_{41}^*\rho_{14} + ig_{41}\rho_{41}, \quad (1a)$$

$$\begin{aligned} \dot{\rho}_{22} = & -2\gamma_{23}\rho_{22} + 2\gamma_{42}\rho_{44} - 2\Lambda\rho_{22} + 2\Lambda\rho_{33} \\ & + ig_p^*\rho_{32} - ig_p\rho_{23} - ig_{42}^*\rho_{24} + ig_{42}\rho_{42}, \end{aligned} \quad (1b)$$

$$\dot{\rho}_{33} = 2\gamma_{13}\rho_{11} + 2\gamma_{23}\rho_{22} + 2\Lambda\rho_{22} - 2\Lambda\rho_{33} - ig_p^*\rho_{32} + ig_p\rho_{23}, \quad (1c)$$

$$\dot{\rho}_{12} = -(\Gamma_{12} + i\Delta_{41} - i\Delta_{42} + \Lambda)\rho_{12} - ig_{42}^*\rho_{14} - ig_p\rho_{13} + ig_{41}\rho_{42}, \quad (1d)$$

$$\dot{\rho}_{13} = -(\Gamma_{13} + i\Delta_{41} - i\Delta_{42} - i\Delta_p + \Lambda)\rho_{13} - ig_p^*\rho_{12} + ig_{41}\rho_{43}, \quad (1e)$$

$$\dot{\rho}_{14} = -(\Gamma_{14} + i\Delta_{41})\rho_{14} - ig_{41}\rho_{11} + ig_{41}\rho_{44} - ig_{42}\rho_{12}, \quad (1f)$$

$$\dot{\rho}_{23} = -(\Gamma_{23} - i\Delta_p + 2\Lambda)\rho_{23} - ig_p^*\rho_{22} + ig_p^*\rho_{33} + ig_{42}\rho_{43}, \quad (1g)$$

$$\dot{\rho}_{24} = -(\Gamma_{24} + i\Delta_{42} + \Lambda)\rho_{24} - ig_{42}\rho_{22} + ig_{42}\rho_{44} + ig_p^*\rho_{34} - ig_{41}\rho_{21}, \quad (1h)$$

$$\dot{\rho}_{34} = -(\Gamma_{34} + i\Delta_p + i\Delta_{42} + \Lambda)\rho_{34} + ig_p\rho_{24} - ig_{41}\rho_{31} - ig_{42}\rho_{32}, \quad (1i)$$

$$\rho_{44} = 1 - \rho_{11} - \rho_{22} - \rho_{33}. \quad (1j)$$

In the above equations,  $\Gamma_{ij} = (2\gamma_i + 2\gamma_j)/2$  are the damping rates of the coherences with  $\gamma_i$  being the total decay rate out of state  $|i\rangle$ , and  $\Delta_p = \Delta_{23}$  is the probe field detuning.

Our main observable is the response of the atomic medium to the probe field. As will be discussed in Sec. 2.2, the linear susceptibility of the weak probe field is determined by the probe transition coherence  $\rho_{23}$ . We therefore proceed by solving the above equations (1a)-(1i) in the steady state under the assumption of specific parameter relations.

First, in the absence of the incoherent pump field ( $\Lambda = 0$ ), an expansion of the steady state coherence  $\rho_{23}$  to the leading order in the probe field Rabi frequency  $g_p$  yields

$$\rho_{23} = \frac{-g_p(|g_{41}|^2 - C_{13} \cdot C_{34})}{|g_{41}|^2 C_{23} + C_{13}(|g_{42}|^2 - C_{23} \cdot C_{34})}, \quad (2a)$$

$$C_{13} = \Delta_p - \Delta_{41} + \Delta_{42} + i\Gamma_{13}, \quad (2b)$$

$$C_{34} = \Delta_p + \Delta_{42} + i\Gamma_{34}, \quad (2c)$$

$$C_{23} = \Delta_p + i\Gamma_{23}. \quad (2d)$$

It will turn out that an interesting parameter range for the present study is given by

$$\Delta_{41} = \Delta_{42} = 0, \quad (3a)$$

$$\Delta_p \ll \gamma_{31}, \gamma_{41}, \gamma_{42}, \quad (3b)$$

$$g_{41} \ll g_{42}, \quad (3c)$$

$$\gamma_{13} = 0. \quad (3d)$$

In this limit, equation (2a) becomes

$$\rho_{23} = \frac{-g_p(|g_{41}|^2 - i\Delta_p\Gamma_{34})}{|g_{42}|^2\Delta_p + i[|g_{41}|^2\Gamma_{23} - \Delta_p^2(\Gamma_{34} + \Gamma_{23})]}. \quad (4)$$

An inspection of equation (4) reveals that the imaginary part is strictly positive, and the half width of the absorption peak around  $\Delta_p = 0$  is determined by

$$w \simeq \left(\frac{g_{41}}{g_{42}}\right)^2 \Gamma_{23} = \left(\frac{g_{41}}{g_{42}}\right)^2 \gamma_{23}. \quad (5)$$

Next, we seek the corresponding steady state solution for  $\rho_{23}$  with incoherent pump field with pump intensity  $\Lambda$ . The parameters are chosen to satisfy equations (3a)-(3d) as well as the new condition on the pump field

$$\Lambda_0 \ll \Lambda \ll \gamma_{41}, \gamma_{42}. \quad (6)$$

Further, we assume the Rabi frequencies  $g_{ij}$  to be real in the following. We obtain in leading order of the probe field coupling  $g_p$

$$\rho_{23} = \frac{g_{41}^2 g_p \gamma_{23}}{(g_{42}^2 \gamma_{23} + 2\Lambda \Gamma_{24} \gamma_{42})} \frac{\Delta_p - i\Lambda}{\Delta_p^2 + \Lambda^2}. \quad (7)$$

Here the parameter  $\Lambda_0$  is defined by

$$\Lambda_0 = \frac{g_{41} \gamma_{23} (\gamma_{41} + \gamma_{23})}{g_{42}^2 \gamma_{41} + \gamma_{23} \Gamma_{34} (\gamma_{41} + \gamma_{23})} \simeq \left(\frac{g_{41}}{g_{42}}\right)^2 \gamma_{23}. \quad (8)$$

Since  $|g_{41}/g_{42}|^2\gamma_{23}$  can be made small, for a suitable combination of the Rabi frequencies  $g_{41}$  and  $g_{42}$  the condition  $\Lambda \gg \Lambda_0$  can be fulfilled even for incoherent pump strengths which are orders of magnitude smaller those required, e.g., to saturate the optical transition.

We find that the imaginary part of equation (7) is negative if the condition  $\Lambda \gg \Lambda_0$  is fulfilled. Thus  $\Lambda_0$  indicates the incoherent pumping rate at which the absorption peak turns into a gain structure, if the conditions in equations (3a)-(3d) and (6) are fulfilled.

## 2.2. Observables

Our main observable is the response of the atomic medium to the probe field. The linear susceptibility of the weak probe field can be written as [28]

$$\chi(\omega_p) = \frac{2N\eta_p}{\epsilon_0 E_p} \rho_{23}(\omega_p), \quad (9)$$

where  $N$  is the atom number density in the medium,  $\eta_p$  is the probe transition dipole moment and  $\chi = \chi' + i\chi''$ . The real and imaginary parts of  $\chi(\omega_p)$  correspond to the dispersion and the absorption, respectively. The slope of the dispersion with respect to the probe detuning has a major role in the calculation of the group velocity. We introduce the group index,  $n_g = c/v_g$ , where the group velocity  $v_g$  of the probe field is given by [10, 13]

$$v_g = \frac{c}{\left[1 + 2\pi\chi'(\omega_p) + 2\pi\omega_p \frac{\partial\chi'(\omega_p)}{\partial\omega_p}\right]}. \quad (10)$$

Equation (10) implies that, for a negligible real part  $\chi'(\omega_p)$ , the group velocity can be significantly reduced via a steep positive dispersion. Strong negative dispersion, on the other hand, can lead to an increase in the group velocity and even to a negative group velocity.

Substituting equations (7) and (9) in equation (10), the group index of the probe field evaluates to

$$n_g - 1 = \frac{g_{41}^2 g_p \gamma_{23}}{(g_{42}^2 \gamma_{23} + 2 \Lambda \Gamma_{24} \gamma_{42}) (\Delta_p^2 + \Lambda^2)^2}. \quad (11)$$

It can be expected from equation (11) that for suitable parameters, the group index around  $\Delta_p = 0$  is negative and accompanied by gain, and this is indeed what we find below.

The relation between coherence and susceptibility equation (9) can be rewritten as

$$\chi(\omega_p) = \frac{2N\eta_p}{\epsilon_0 E_p} \rho_{23}(\omega_p) = \frac{3N\lambda_p^3}{4\pi^2} \frac{\gamma_{23}}{\gamma} \frac{\rho_{23}(\omega_p)}{g_p/\gamma}, \quad (12)$$

where we have used  $\gamma_{23} = (\eta_p^2 \bar{\omega}_{23}^3)/(3\pi\epsilon_0 \hbar c^3)$  and  $g_p = \eta_{23} E_p/\hbar$  as well as  $\omega_{23} = 2\pi c/\lambda_{23}$  with the probe transition wavelength  $\lambda_{23}$ . For mercury probe wavelength 253.7 nm, particle density  $N = 10^{12} \text{cm}^{-3}$  and  $\gamma_{23}/\gamma = 0.14$  as found in mercury one finally obtains

$$\chi(\omega_p) = 1.74 \times 10^{-4} \frac{\rho_{23}(\omega_p)}{g_p/\gamma}. \quad (13)$$

Throughout our discussion of numerical results, we will assume these parameters in order to evaluate the susceptibility.

### 2.3. Dressed-state analysis

We now introduce the dressed states generated by the strong driving field acting on transition  $|2\rangle \leftrightarrow |4\rangle$  and the coupling field acting on transition  $|1\rangle \leftrightarrow |4\rangle$ , in order to demonstrate the presence of interacting dark resonances due to the perturbing field with Rabi frequency  $g_{41}$  [27]. In the absence of the incoherent pump field, the dressed states are

$$|0\rangle = -\frac{g_{42}}{\sqrt{g_{41}^2 + g_{42}^2}} |1\rangle + \frac{g_{41}}{\sqrt{g_{41}^2 + g_{42}^2}} |2\rangle, \quad (14a)$$

$$|\pm\rangle = \frac{g_{41}}{\sqrt{2(g_{41}^2 + g_{42}^2)}} |1\rangle + \frac{g_{42}}{\sqrt{2(g_{41}^2 + g_{42}^2)}} |2\rangle \mp \frac{1}{\sqrt{2}} |4\rangle, \quad (14b)$$

with energies

$$\lambda_0 = 0, \quad \lambda_{\pm} = \pm \hbar \sqrt{g_{41}^2 + g_{42}^2}. \quad (15)$$

The two dressed states  $|\pm\rangle$  correspond, in the limit of vanishing driving field  $g_{41}$ , to the usual Autler-Townes dressed components split by  $2\hbar g_{42}$ . The third dressed state  $|0\rangle$  coincides in this limit with the bare state  $|1\rangle$  and hence is decoupled from the fields. This is no longer so in the presence of a second weak driving field  $g_{41}$ . In this case the dressed state  $|0\rangle$  contains an admixture of  $|2\rangle$  and thus has a nonzero dipole matrix element

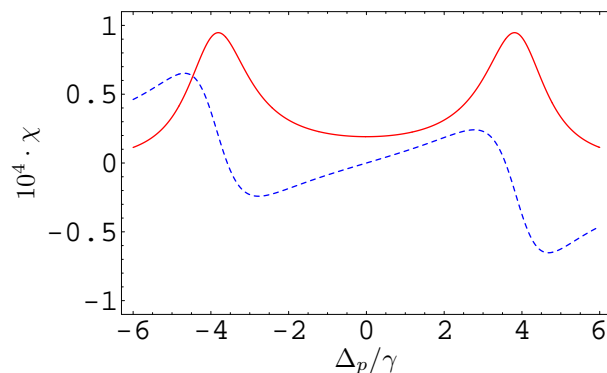


**Figure 2.** Real (blue dashed) and imaginary (red solid) parts of the susceptibility  $\chi$  as a function of the probe detuning  $\Delta_p$  for the parameters  $\gamma_{41} = \gamma$ ,  $\gamma_{23} = 0.14\gamma$ ,  $\gamma_{42} = 0.79\gamma$ ,  $\gamma_{13} = 0.01\gamma$ ,  $g_p = 10^{-4}\gamma$ ,  $g_{41} = 0$ ,  $g_{42} = 4\gamma$ ,  $\Lambda = 0$ ,  $\Delta_{42} = \Delta_{41} = 0$ .

with the state  $|3\rangle$ . As a result of this coupling, there are transitions between  $|0\rangle$  and  $|3\rangle$ , corresponding to three photon resonances from  $|1\rangle$  to  $|3\rangle$  that exhibit interference effects [27].

### 3. Results

In figure 2 we show the real (blue dashed) and imaginary (red solid) part of the probe field susceptibility  $\chi$  versus the probe detuning  $\Delta_p$ , which correspond to the dispersive and absorptive properties of the medium, respectively. In this figure, the perturbing laser field is switched off,  $g_{41} = 0$ . The other parameters are  $\gamma_{41} = \gamma$ ,  $\gamma_{23} = 0.14\gamma$ ,  $\gamma_{42} = 0.79\gamma$ ,  $\gamma_{13} = 0.01\gamma$ ,  $g_p = 10^{-4}\gamma$ ,  $g_{42} = 4\gamma$ ,  $\Lambda = 0$ ,  $\Delta_{42} = \Delta_{41} = 0$ . Note that the ratios of the decay rates correspond to the case found in mercury, see figure 1(b). We have added a weak decay rate  $\gamma_{13}$ , since otherwise in the steady state all population is trapped in  $|3\rangle$ . The driving field with Rabi frequency  $g_{42}$  leads to an Autler-Townes doublet with a dip in the absorption at zero detuning, i.e., partial electromagnetically induced transparency (EIT). The slope of the real part of the susceptibility in the region of reduced absorption is positive. We thus find that subluminal light propagation occurs around zero detuning with reduced absorption as it is common for EIT. If the state  $|4\rangle$  was long-lived, then the EIT leading to the partial transparency would be more pronounced such that the absorption would vanish at zero detuning.

In figure 3, in addition we apply the weak perturbing field with Rabi frequency  $g_{41} = 0.04\gamma$ , and assume negligible decay on transition  $|3\rangle \leftrightarrow |1\rangle$ , since a trapping in this state is now avoided by the additional laser field. The results are identical to figure 2 except for a narrow absorption spike at around zero detuning. The shape and width of the absorption spike are determined by equation (2a) and equation (5), respectively. In particular, the width is much less than the natural linewidth. Again, for a long-lived state  $|4\rangle$ , the transparency regions on each side of the absorption spike would become two points of EIT, i.e., a double dark state [26]. In terms of the light propagation, the slope of the real part of the susceptibility around zero detuning is negative such that

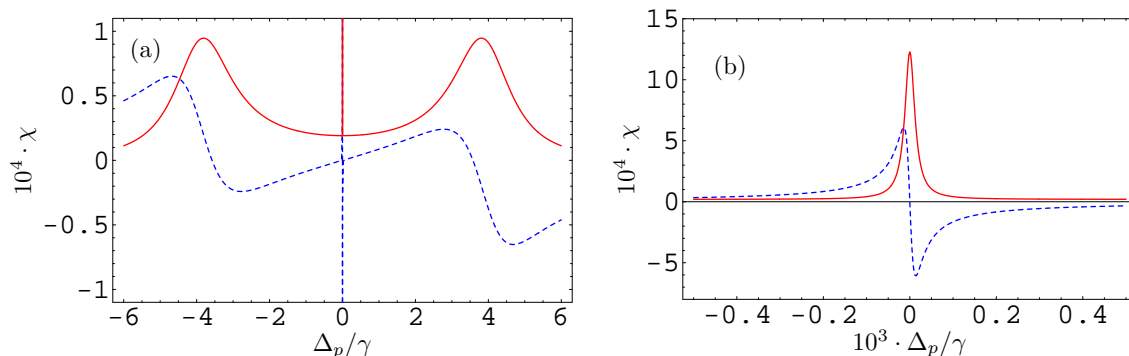


**Figure 3.** Real (blue dashed) and imaginary (red solid) parts of the susceptibility  $\chi$  as a function of the probe detuning for  $\gamma_{13} = 0$  and  $g_{41} = 0.04\gamma$ . The other parameters are the same as in figure 2. (b) is a closeup on the central part of (a).

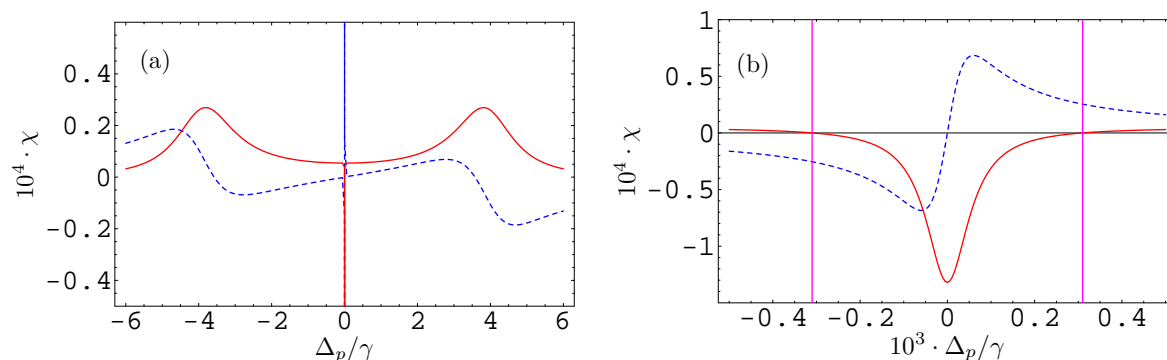


**Figure 4.** Real (blue dashed) and imaginary (red solid) parts of the susceptibility  $\chi$  as a function of the probe detuning for  $\Lambda = 4 \times 10^{-5}\gamma$ . The other parameters are the same as in figure 3. (b) is a closeup on the central part of (a). The purple vertical lines indicate the roots of the imaginary part.

superluminal light propagation could be observed, albeit with high absorption.

We now in addition apply a weak incoherent pumping field on the probe transition  $|2\rangle - |3\rangle$ . Figure 4 shows the corresponding results. The incoherent pump field rate is chosen as  $\Lambda = 4 \times 10^{-5}\gamma$ . In this case, the superluminal light propagation found in figure 3 at  $\Delta_p = 0$  switches to subluminal propagation, and the absorption spike at zero detuning becomes a gain spike. The shape of the gain spike is determined by the imaginary part of equation (7) which is Lorentzian with halfwidth equal to  $\Lambda$ . This can be understood from the fact that the spike arises from a three-photon transition from  $|1\rangle$  to  $|3\rangle$ . In the absence of the incoherent pump field, most of the population is in level  $|3\rangle$ . Therefore, the probe field is absorbed. But in the presence of the weak incoherent pump field, the population is transferred to level  $|1\rangle$ . This optical pumping leads to the gain spike in the spectrum.

Furthermore, it can be seen from Fig. 4 that at  $\Delta_p \approx \pm 3.1 \times 10^{-4}\gamma$  (indicated by the purple vertical lines), the imaginary part of the susceptibility vanishes together with a negative slope of the real part. At these probe field detunings, the real part of



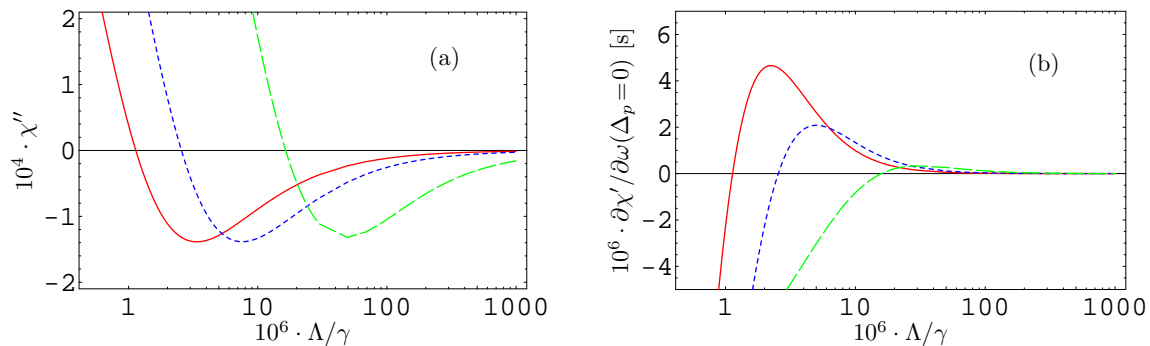


**Figure 5.** (a) Imaginary part  $\chi''$  of the susceptibility as a function of the pumping field strength  $\Lambda$ . The parameters are as in figure 3 with  $\Delta_p = 0$ , and  $g_{42} = 15\gamma$  (solid red),  $10\gamma$  (short-dashed blue),  $4\gamma$  (long-dashed green). (b) Slope of the real part  $\chi'$  of the susceptibility at zero probe field detuning  $\Delta_p = 0$  for parameters as in (a).

the susceptibility itself is non-zero, and is negative (positive) for  $\Delta_p \approx -3.1 \times 10^{-4}\gamma$  ( $\Delta_p \approx -3.1 \times 10^{-4}\gamma$ ). In the following, we discuss the two cases of interest with resonant or non-resonant probe field separately.

We start with the resonant case  $\Delta_p = 0$ . In figure 5(a), we study the effect of the incoherent pumping strength  $\Lambda$  on the magnitude of the imaginary part of the susceptibility  $\chi$  at resonance  $\Delta_p = 0$ . It can be seen that depending on the coupling field Rabi frequency  $g_{42}$ , the transition from absorption to gain occurs at different values of the incoherent pumping. For the parameters of figure 3, which correspond to the long-dashed green curve in figure 5(a), the transition is at about  $\Lambda \approx 2 \times 10^{-5} \gamma$ . This explains why gain could be observed for the parameters in figure 4. On increasing the incoherent pumping further, the imaginary part approaches zero again.

After the discussion of the absorption, we now turn to a discussion of our main observable, the group velocity. Since the real part of  $\chi$  itself vanishes at  $\Delta_p = 0$ , the group velocity is determined by the slope of the real part of the susceptibility at  $\Delta_p = 0$ , see equation (10). This quantity is shown in figure 5(b). It can be seen that, for no or small incoherent pumping, the system exhibits a negative slope, which leads to a superluminal or even negative group velocity. On increasing  $\Lambda$ , the slope can be adjusted to large positive values, where subluminal light can be expected. Thus in principle the system allows for a wide range of group velocities, controlled via the incoherent pump rate  $\Lambda$ . But from a comparison of figures 5 (a) and (b) it can be seen that typically negative slopes are accompanied by absorption, while positive slopes occur together with gain. Thus at  $\Delta_p \approx 0$ , only a reduction of the group velocity is accessible in experiments without absorption. The different curves in figure 5 further show that the precise response of the system to the incoherent pumping can be controlled by varying the coupling field Rabi frequency  $g_{42}$ . In particular, stronger coupling fields  $g_{42}$  may be favourable, since then the range of possible slopes is increased, as can be seen from figure 5(b).

We now turn to a discussion of the non-resonant case,  $\Delta_p \neq 0$ , and focus on the

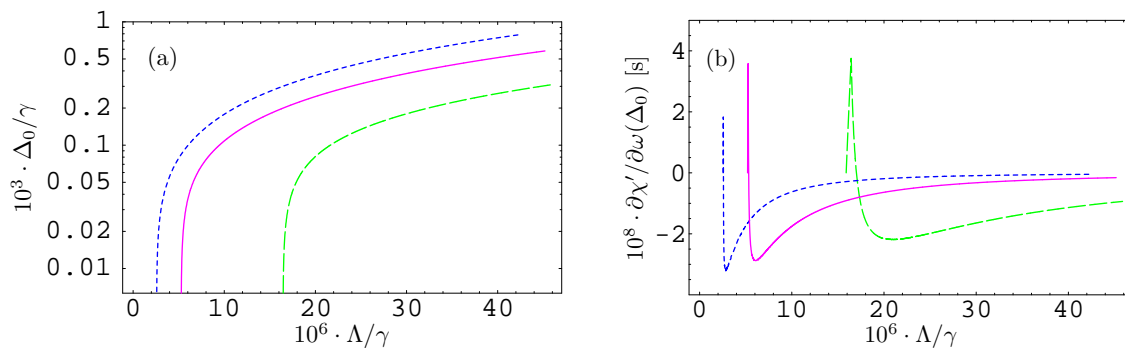


**Figure 6.** (a) Position  $\Delta_0$  of the root of the imaginary part of the susceptibility  $\chi$  as a function of the pumping field strength  $\Lambda$ . At this frequency, light passes unattenuated through the medium. (b) Slope of the real part  $\chi'$  of the susceptibility at the detuning  $\Delta_0$  with vanishing absorption. The parameters are as in figure 3 but with  $g_{42} = 10\gamma$  (short-dashed blue),  $g_{42} = 7\gamma$  (solid purple), and  $g_{42} = 4\gamma$  (long-dashed green).

regions with vanishing absorption, such as  $\Delta_p \approx \pm 3.1 \times 10^{-4}\gamma$  in figure 4. It can be seen that around these probe field detunings, the imaginary part of the susceptibility vanishes, such that the probe field passes unattenuated through the medium. At the same time, the real part of the susceptibility is non-zero, and has a negative slope. Therefore, at these frequencies, superluminal or negative group velocities are accessible without absorption. In order to study this result in more detail, in figure 6(a) we show the probe field detuning  $\Delta_0$  at which the imaginary part of the susceptibility vanishes as a function of the incoherent pumping rate  $\Lambda$ . It can be seen that for no or small incoherent pumping  $\Lambda$ , there is always absorption such that no  $\Delta_0$  can be found. Once  $\Lambda$  is large enough for a root in the imaginary part of the susceptibility to occur, the position of the root first increases rapidly with  $\Lambda$ , and then saturates. The required value of  $\Lambda$  also depends on the strength of the coupling field  $g_{42}$  as can be seen from figure 6(a).

The corresponding figure 6(b) depicts the slope of the real part of the susceptibility as a function of  $\Lambda$ . It can be seen that by varying the pump field strength  $\Lambda$ , both positive and negative slopes can be achieved at frequencies where the medium absorption is zero. After passing through a maximum positive slope, the slope drops to a minimum negative slope and then slowly increases again towards vanishing slope. For every value of the coupling field Rabi frequency  $g_{42}$ , optimum values of  $\Lambda$  can be identified where the slope is steepest and either positive or negative. The maximum absolute values of the slope are of order  $10^{-8} \text{ s}^{-1}$ , such that the third term  $2\pi\omega_p \partial\chi'/\partial\omega$  in the denominator of equation (10) for our probe transition varies between approximately  $-10^9$  and  $+10^9$ . Therefore, strongly sub- and superluminal propagation as well as a large range of negative group velocities occur without absorption in our sample, controlled by the magnitude of the incoherent pumping. It should be noted that only very weak incoherent pumping is required, as can be seen from the scaling of the x-axes in figures 6.

Throughout this section, the figures 2-6 have been obtained from a numerical

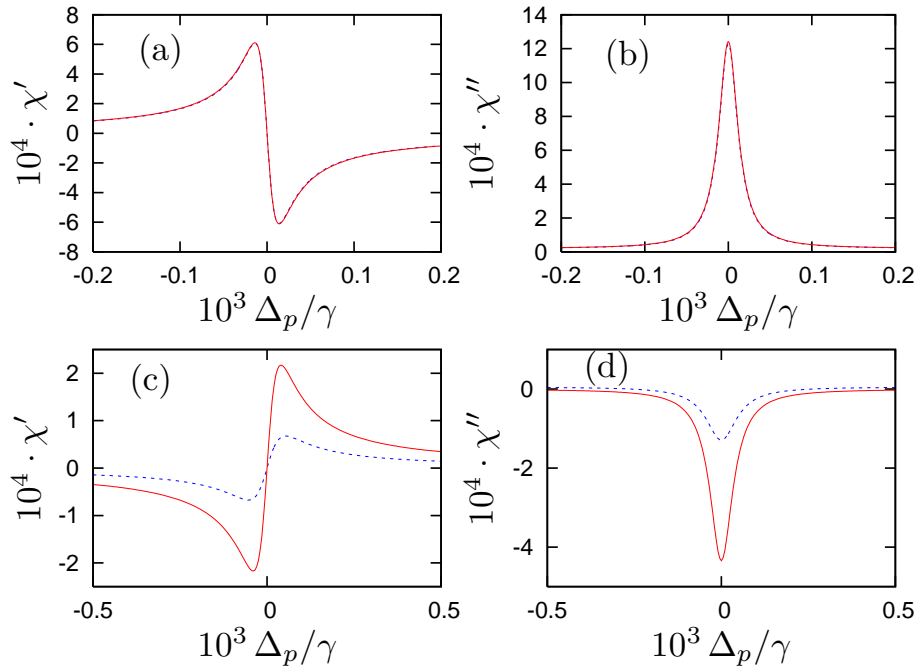


**Figure 7.** Real (a,c) and imaginary (b,d) parts of the susceptibility  $\chi$  as a function of the probe detuning. The analytical results are shown as solid red lines, whereas our numerical results are shown as dashed blue lines. The parameters in (a,b) are as in figure 3, and equation (4) is shown as the analytical result. The parameters in (c,d) are as in figure 4, with equation (7) as analytical result.

solution of the full density matrix equations (1a)-(1i). In the following, we verify our approximate analytical expressions, equations (2a)-(7), by a comparison to the exact numerical calculations. The result is shown in figure 7, where the solid red curves correspond to the approximate analytical solutions, whereas the blue dashed curves represent our numerical results. The approximate result equation (4) for the case without incoherent pump field is shown in comparison to the numerical data in figure 7(a,b). It turns out that in this case, the results from equation (4) are virtually identical to the corresponding numerical results. Equation (7) for the case with incoherent pumping is compared to the numerical results in figure 7(c,d). Here, the analytic results only describe the qualitative behavior of the curves. The reason for this is that in this figure, we chose parameters for which the condition  $\Lambda \gg \Lambda_0$  in equation (6) is not well satisfied. If the incoherent pumping  $\Lambda$  is increased, the agreement of the approximate results with the numerical calculation improves. Thus we conclude that our analytical results describe the system well enough to allow for an optimization of the parameters towards a desired peak structure, as long as the conditions on the parameters are satisfied.

## 4. Conclusion

We have discussed the dispersive and absorptive properties of a four-level atomic medium that exhibits interacting dark-state resonances. In our numerical analysis, we have focused on mercury atoms with an ultraviolet probe field wavelength of 243.7 nm. Due to the interacting resonances, a high-resolution structure appears in both the absorption and the dispersion spectra. A weak probe field tuned to this resonance usually experiences superluminal propagation with absorption. But if in addition a weak incoherent pump field is applied to the probe transition, then the superluminal light propagation changes to subluminal light propagation accompanied by no absorption or gain. Slightly off resonance, the probe field experiences a vanishing imaginary part of the susceptibility. At these off-resonant frequencies, the real part of the susceptibility itself is non-zero and has a slope depending on the incoherent pumping strength. Thus both sub- and superluminal light propagation as well as negative group velocities can be achieved without absorption. The control via the incoherent pump fields suggests potential applications, e.g., in optical switching devices or in controllable pulse delay lines for the ultraviolet frequency region.

## Acknowledgments

MM gratefully acknowledges support for this work from the German Science Foundation and from Zanjan University, Zanjan, Iran.

## References

- [1] Ficek Z and Swain S 2004 *Quantum coherence and interference: Theory and Experiments* (Springer, Berlin)
- [2] Sommerfeld A 1907 *Z. Phys.* **8** 841
- [3] Brillouin L 1960 *Wave propagation and group velocity* (Academic Press, New York)
- [4] Harris S E, Field J E, and Kasapi A 1992 *Phys. Rev. A* **46** R29; Kasapi A, Jain M, Yin G Y, and Harris S E 1995 *Phys. Rev. Lett.* **74** 2447
- [5] Schmidt O, Wynands R, Hussein Z, and Meschede D 1996 *Phys. Rev. A* **53** R27; Muller G, Wicht A, Rinkleff R, and Danzmann K 1996 *Opt. Commun.* **127** 37
- [6] Field J E, Hahn H, and Harris S E 1991 *Phys. Rev. Lett.* **67** 3062; Harris S E, Field J E, and Imamoglu A 1990 *Phys. Rev. Lett.* **64** 1107; Harris S E 1997 *Phys. Today* **50** 36
- [7] Xiao M, Li Y Q, Jin S Z, and Gea-Banacloche J 1995 *Phys. Rev. Lett.* **74** 666; Budker D, Kimball D F, Rochester S M, and Yashchuk V V 1999 *Phys. Rev. Lett.* **83** 1767
- [8] Agarwal G S and Dey T N 2004 *Phys. Rev. Lett.* **92**, 203901
- [9] Patnaik A K, Kien F L, and Hakuta K 2004 *Phys. Rev. A* **69**, 035803
- [10] Hau L V, Harris S E, Dutton Z and Behroozi C H 1999 *Nature (London)* **394**, 594
- [11] Kash M M, Sautenkov V A, Zihrov A S, Hollberg L, Welch G R, Lukin M D, Rostovtsev Y, Fry E S and Scully M O 1999 *Phys. Rev. Lett.* **82** 5229; Ham S B, Hemmer P R and Shahriar M S 1997 *Opt. Commun.* **144** 227
- [12] Steinberg A M and Chiao R Y 1994 *Phys. Rev A* **49** 2071; Bolda E L, Garrison J C, Chiao R Y 1994 *Phys. Rev. A* **48** 2938
- [13] Wang L J, Kuzmich A and Dogariu A 2000 *Nature (London)* **406** 277; Dogariu A, Kuzmich A and Wang L J 2001 *Phys. Rev. A* **63**, 053806; Kuzmich A, Dogariu A, Wang L J, Millonni P M

- and Chiao R Y 2001 Phys. Rev. Lett. **86**, 3925; Dogariu A, Kuzmich A, Cao H and Wang L J 2003 Opt. Express. **8** 344
- [14] Chiao R Y and Steinberg A M, in: *Progress in Optics XXXVII*, ed. E. Wolf (Elsevier, Amsterdam, 1997) p.345.
- [15] Kim K, Moon H S, Lee C, Kin S K, and Kin J B 2003 Phys. Rev. A **68** 013810
- [16] Goren C, Wilson-Gordon A D, Rosenbluh M, and Friedmann H 2003 Phys. Rev. A **68** 043818
- [17] Agarwal G S, Dey T N and Menon S 2001 Phys. Rev. A **64** 053809
- [18] Han D, Guo H, Bai Y, and Sun H 2005 Phys. Lett. A **334** 243
- [19] Tajalli H, and Sahrai M 2005 J. Opt. B: Quantum Semiclassical Opt. **7** 168
- [20] Bortman-Arbiv D, Wilson-Gordon A D, and Friedmann H 2001 Phys. Rev. A **63** 043818
- [21] Morigi G, Franke-Arnold S and Oppo G L 2002 Phys. Rev. A **66** 053409
- [22] Zhang J, Hernandez G, and Zhu Y 2006 Opt. Lett. **31** 2598
- [23] Mahmoudi M, Sahrai M and Tajalli H 2006 J. Phys. B **39** 1825
- [24] Mahmoudi M, Sahrai M and Tajalli H 2006 Phys. Lett. A **357** 66
- [25] Mahmoudi M and Evers J 2006 Phys. Rev. A. **74** 063827
- [26] Lukin M D, Yelin S F, Fleischhauer M and Scully M O 1999 Phys. Rev. A **60** 3225
- [27] Fry E S, Lukin M D, Walther T, and Welch G R 2000 Opt. Commun. **179** 499
- [28] Scully M O and Zubairy M S 1997 *Quantum Optics* (Cambridge University Press, Cambridge)